

# Pathways of Microvascular Permeability in the Synovium of Normal and Diseased Human Knees

PETER A. SIMKIN and JOHN E. BASSETT

**ABSTRACT. Objective.** Our study uses the entire proteomes of serum and synovial fluid (SF) to characterize the avenues of microvascular egress of plasma proteins, and quantifies that traffic in normal and diseased human knees.

**Methods.** Paired aliquots of serum and SF were collected from 17 knees of 11 subjects who died without evident joint disease and 16 patients with clinical effusions, fractionated by gel filtration chromatography and analyzed as continuous plots of the SF/serum concentration ratio versus molecular radius from 1 to 12 nanometers (nm). Curve-stripping methodology, a 3-pore model, and known protein kinetics were then applied to estimate the dimensions of and the net outflow through fenestral, “small,” and “large” apertures in the microvascular endothelium.

**Results.** The 3-pore model correlated highly with the observed data ( $r = 0.992$  in normal and  $0.980$  in arthritis), yielding the following mean values: for the fenestra, the normal radius (nm) was 1.75 and the effused 3.5, and the normal flow ( $\mu\text{l}/\text{min}$ ) was 1.74 and the arthritic 22.0; for the small pore, the normal radius was 8.6 and the effused 8.5, and the normal flow was 1.5 and the arthritic flow 9.1; for the large pore, the normal radius was 40 and the effused 36, and the normal flow was 0.24 and the arthritic flow 15.5.

**Conclusion.** These findings provide the first functional definition of synovial, endothelial fenestrae; reveal that the “increased vascular permeability” of inflammation is not limited to interendothelial gaps; present evidence suggesting that glycocalyx damage and aquaporin upregulation may affect permeability in arthritic synovium; and define a straightforward methodology for interpretation of biomarker concentrations in arthritic SF. (J Rheumatol First Release Nov 1 2011; doi:10.3899/jrheum.110785)

## Key Indexing Terms:

ENDOTHELIUM  
PROTEOME

FENESTRA  
AQUAPORIN

BIOMARKERS  
GLYCOCALYX

Synovial fluid (SF) is not the finished product of a synovial organ as bile and urine are the products of the liver and the kidney. Instead, it is a vital tissue fluid whose constituents are continually cleared and replenished in an ongoing equilibrium with the perfusing plasma. For small molecules (such as oxygen, water, urea, and urate) this interchange is not just an equilibrium, it is a full equilibration. These solutes cross and recross the vascular endothelium at rates inversely proportional to their size; but the barrier is highly permeable, the rates are rapid, and the concentrations remain essentially the same in SF as they are in plasma<sup>1</sup>.

The situation is different for the proteins of SF. They too are transitory visitors moving from and to the plasma, but the endothelial barrier is much more restrictive, their stay in the joint is measured better in hours than in minutes, and they

return to the circulation by lymphatics rather than the microvasculature<sup>2</sup>.

In contrast to the selective, sieving entry into the joint, the lymphatic outflow path does not discriminate by size; large proteins (such as 19S IgM) leave as fast as small ones (such as albumin); the exit becomes restrictive only to megamolecules (such as hyaluronan)<sup>3,4,5,6</sup>. These opposing processes of restricted ingress and open egress result in a concentration gradient ranging from full equilibration of very small plasma proteins (such as insulin) to near exclusion of the large in normal SF.

We report studies using gel filtration chromatography to examine this gradient in fluids from normal and diseased human knees. The resulting essentially continuous records of SF to serum concentration ratios (SF/S) are then analyzed with existing kinetic data and clearance concepts to characterize the porosity of the endothelial barrier in synovial microvessels. The findings fit well with a 3-pore model. The smallest pore, with a radius ( $r$ ) of 1.75 nanometers (nm) in normal subjects, permits the highest rate of exchange and is thought to lie in or above endothelial fenestrations. The next,  $r = 8.6$  nm, permits paracellular flow through the presumed cadherin junctions between adjacent cells. The largest pores,  $r \sim 36$  nm (which may represent connecting “caveolae” in nor-

*From the Division of Rheumatology, University of Washington, Seattle, Washington, USA.*

*Supported in part by US National Institutes of Health grant RO1 AM32811.*

*P.A. Simkin, MD; J.E. Bassett, PhD, Division of Rheumatology, University of Washington.*

*Address correspondence to Dr. P. Simkin, Division of Rheumatology, Box 356428, University of Washington, Seattle, WA 98195, USA.*

*E-mail: psimkin@uw.edu*

*Accepted for publication July 15, 2011.*

Personal non-commercial use only. The Journal of Rheumatology Copyright © 2011. All rights reserved.

mal tissue), become plentiful in arthritis in accord with classic concepts of plasma leakage caused by “unzipping” of cellular junctions by inflammatory mediators. The 8.6-nm pore does not change with arthritis but the apparent fenestral pore widens, perhaps reflecting inflammation-induced changes in the overlying glycocalyx or release of byproducts of synovial inflammation. Findings in some effusions suggest the appearance of aquaporin channels that serve as “water-only” fourth pores.

## MATERIALS AND METHODS

**Clearance approach.** Unlike the linings of other body cavities (peritoneum, pleural space, etc.) the synovium lacks a mesothelial surface with an underlying basement membrane<sup>7</sup>. As a result, molecules passing between the synovial cells encounter only the tissue interstitium as they move back and forth between the joint space and the microvasculature. The relevant vessels comprise the perfusing capillaries and the draining lymphatics, both of which lie close to the synovial surface. In fact, the terminal lymphatics are so shallow that small and large proteins are cleared from the joint at the same flow rate, i.e., the passage from SF to lymph is not size-selective<sup>3,4,5</sup>. This finding facilitates analysis of protein kinetics by the classic concept of clearance (C): the volume/min of serum ( $C_s$ ) or synovial fluid ( $C_{sf}$ ) that is cleared of a given solute<sup>2</sup>.

We assume a state of equilibrium at the time of aspiration. By definition, this means that the flux rate (F) for each protein entering the knee from the plasma ( $F_{in}$ ) equals its rate of departure from the articular cavity ( $F_{out}$ ). With flux (measured, for instance, in mg/min) being the product of concentration (mg/ml) and clearance (ml/min), these rates may be written:

$$F_{in} = S \times C_s \text{ and } F_{out} = SF \times C_{sf}$$

Because  $F_{in} = F_{out}$ , ( $S \times C_s$ ) will equal ( $SF \times C_{sf}$ ), and these terms may be reexpressed as  $SF/S = C_s/C_{sf}$ . Given that  $C_{sf}$  is invariant in each person’s knee across the relevant range of SF/S determinations, the formula

$$C_s = SF/S \times C_{sf}$$

may then be applied to determine the clearance rate (in ml/min or  $\mu$ l/min) at which proteins of any size pass from plasma into synovial fluid. We applied this simple formula to our chromatographic determinations of mean SF/S over a continuous range of molecular radii between 1 and 12 nm. The SF/S data were multiplied by  $C_{sf}$  values derived from previous studies of articular kinetics to exemplify the influx of plasma proteins into normal and diseased human knees<sup>2</sup>.

**Specimens.** Seventeen normal samples of SF were obtained at autopsy from the knees of 11 subjects who died at the University of Washington Medical Center. None had a known rheumatic disease and there was no evidence of arthritis on inspection of the joints or of the synovial aspirates. Wrists, elbows, shoulders, hips, and ankles of each body were also aspirated for total protein determinations in a related study<sup>8</sup>. All aspirations were done within 24 hours of death. Paired sera were obtained from residual samples on hand in the clinical chemistry laboratory. All had been drawn within 24 hours prior to death for studies required in the care of these terminally ill subjects. Previous studies in other species have found that the concentrations of proteins in normal joints within 1 day postmortem are indistinguishable from those in SF aspirates obtained from the same animals *in vivo*<sup>9,10</sup>.

Obviously, dead patients are not normal, and we would not expect normal proteomes in postmortem serum or SF. We do expect, however, that the microvasculature of their knees will have been normal and that balanced, convective transport will lead each protein to a partition reflecting the same apertures present in healthy control subjects.

Pathologic SF aliquots were taken from diagnostic or therapeutic knee aspirations done in the Rheumatology Clinic of the University of Washington Medical Center. Paired serum samples were from aspirates drawn on the same afternoon. The final analysis included 16 fluids from patients with the fol-

lowing diagnoses: rheumatoid arthritis (RA; 5), osteoarthritis (OA; 3), reactive arthritis (2), psoriatic arthritis (3), systemic lupus erythematosus (1), pigmented villonodular synovitis (1), and undifferentiated connective tissue disease (1). All specimens were obtained, studied, and reported in accord with the Helsinki Declaration and approval of the University of Washington institutional review board. Informed consent was not required at the time of collection since all samples were de-identified residual aliquots from laboratory specimens obtained in the course of routine clinical care.

All serum and SF were centrifuged for  $\geq 10$  min at 3000 rpm to remove cells, fibrin clot, and any other particulate matter. Small aliquots of SF, 150  $\mu$ l, were then incubated 1 h with 1  $\mu$ l of 1% hyaluronidase solution (Sigma-Aldrich Corp., St. Louis, MO, USA) at 37°C to lyse hyaluronan.

**Chromatography.** One hundred microliter aliquots of each sample were injected in a Waters HPLC system (Waters 501 pump, Waters UK6 injector, and Waters 490 detector, Waters Corp., Milford, MA, USA) and run at room temperature and low pressure (< 30 mm Hg) over two 1.4  $\times$  30-cm Superose 6 columns (Pharmacia, Uppsala, Sweden) joined in series and protected by a Macrosphere TW300 (Alltech Associates Inc., Deerfield, IL, USA) guard column. Columns were eluted with phosphate buffered physiological saline solution, pH 7.3, at 0.3 ml/min, and effluent optical density was monitored continuously at 280 nm. Each run required 3 h. Serum and SF from the same individual were always run consecutively. Standard curves of retention time on the column versus log molecular radius (mr) for 6 globular marker proteins [bovine thyroglobulin (molecular weight [mw] = 669 kDa, mr = 7.97 nm), equine apoferritin (mw = 443 kDa, mr = 5.75 nm), sweet potato B-amylase (mw = 200 kDa, mr = 5.14 nm), human serum albumin (mw = 69 kDa, mr = 3.43 nm), bovine carbonic anhydrase (mw = 29 kDa, mr = 2.37 nm), and equine cytochrome C (mw = 12 kDa, mr = 1.66 nm)] were run at least every other day, and were invariably linear with correlation coefficients consistently > 0.99 (Figure 1). This range of molecular sizes spans almost all of the proteins in the proteome of normal human serum.

Under the guidance of David Teller, professor of biochemistry at the University of Washington, we determined the mr from the formula  $R = M(1 - \nu\rho)/6N_s\pi\eta$ . M is the known molecular weight, sedimentation coefficient is s, N is Avogadro’s number,  $\nu$  is the partial specific volume,  $\eta$  is the viscosity, and  $\rho$  is the density of the solution. Radii determined from sedimentation coefficients should be more precise than traditional coefficients based on diffusion in porous media.

All optical density and SF/S values were expressed and plotted as a func-

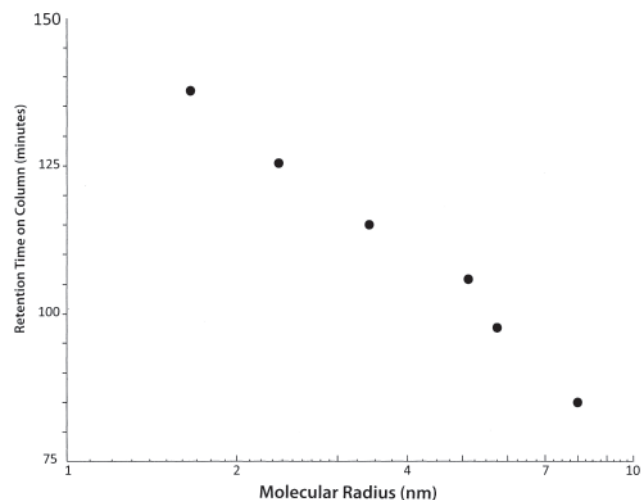


**Figure 1.** Standard curve of column retention time for 6 reference proteins (equine cytochrome C, bovine carbonic anhydrase, human serum albumin, sweet potato  $\beta$ -amylase, equine apoferritin, and bovine thyroglobulin) plotted against the log of their molecular radii. Such plots were consistently linear across this broad range of protein sizes.

tion of  $mr^{11}$ . Control aliquots of hyaluronidase were run over the columns and were indistinguishable from background at 280 nm.

**Analysis.** Plasma and the interstitial fluids derived from it contain thousands of proteins in a continuous range of molecular sizes. Each of these species should elute from a gel filtration column as a simple gaussian curve. Were the curve of any single protein in SF to be factored by that of the same protein in serum, we would expect a plateau at some ratio between 0 and 1. This plateau would be centered over the radius of that protein in a plot of SF/S against molecular size. If not 1 protein but all of them present in serum and SF were so analyzed and plotted, we expected that the theoretical plateaus would merge into a single line depicting the extent of equilibration as a continuous function of protein size. The place of each protein on that line will not depend on its concentration in serum or SF. Instead, it will depend only on its concentration ratio in the expectation that passively determined SF concentrations will reflect those in serum irrespective of whether that concentration is normal or abnormal. The relationships demonstrated in Figure 2 confirm that prediction both in normal SF and in the effusions of patients with arthritis. The analysis is a simple one in theory and in practice, but it nonetheless carries substantial power when its findings are used to examine the physiological barrier between serum and SF.

To determine the pattern of clearance from serum into normal or diseased joints, each curve was multiplied by mean efflux clearance values, i.e., lymph flow, obtained in previous studies with radiolabeled serum albumin in the knees of unanesthetized ambulatory individuals. In previous studies from our Division of Rheumatology of 11 patients with RA and 9 with OA, the mean articular volume was 107 ml and the weighted mean clearance constant was 0.00053/min ( $t_{1/2} = 0.9$  days), yielding an average clearance rate of 57  $\mu\text{l}/\text{min}$  ( $71 \pm 28 \mu\text{l}/\text{min}$  in RA and  $39 \pm 30 \mu\text{l}/\text{min}$  in OA)<sup>12</sup>. We chose to use 57  $\mu\text{l}/\text{min}$  for "arthritis" in full recognition of the varied diseases and levels of disease activity represented among our clinical samples. The clearance of all proteins will be higher in patients with severe synovial inflammation and elevated articular efflux. Conversely, all clearance rates will be progressively lower as milder OA gradually merges into normality<sup>13</sup>.

Specific efflux data were not available from normal knees, but we estimated a volume of 15 ml (slightly larger than the lowest we have found in a mildly osteoarthritic knee), and used the mean clearance constant of 0.000232/min ( $t_{1/2} = 2.1$  days) from 12 normal subjects studied by Rodnan and MacLachlan<sup>3</sup> to calculate a clearance rate of 3.48  $\mu\text{l}/\text{min}$ . These data imply that lymphatic flow increases by more than 16-fold in "arthritic" patients with knee effusions (20-fold in RA and 11-fold in OA).

Concurrently, as we found in our previous studies with tritiated water and radioactive iodide<sup>14</sup>, the mean synovial plasma flow in resting knees does not increase significantly in chronic arthritis, but remains close to 2 ml/min. Thus, roughly 2.8% of the perfusing plasma volume may leave the vasculature to return through lymphatics in arthritis of the knee (3.7% in RA and 1.8% in

effused OA), whereas this filtration fraction is only ~0.2% in the average normal knee.

## RESULTS

**Patterns.** In gel filtration chromatography, the column separates by size alone, with the largest solutes eluting first and smaller molecules following in decreasing sequence. To obtain a more familiar orientation, we reversed this order and plotted our findings from 0 to 12 nm (Figures 2, 3, and 4).

All 17 SF/S patterns from "normal" SF were evaluated together since we could discern no obvious pattern differences reflecting age, sex, cause of death, or total protein concentration in the synovial aspirates. To facilitate the analysis, the continuous SF/S ratios for each individual were averaged over 0.5-nm intervals to yield 23 datapoints throughout the full range of useful values. Geometric means of these values ( $\pm$  SE) are plotted in Figure 2. The smallest polypeptides regularly had SF/S values of 1.0 or more, reflecting full equilibration between plasma and SF. Above a radius of ~1.7 nm (~12 kDa), however, SF/S began a slow decline that continued until a radius of ~8.2 nm (~820 kDa). From ~8.2 nm to ~9.2 nm, SF/S leveled off and then began a small rise. This change, however, was not significant by one-way ANOVA. Throughout the full range of proteins studied, SF/S appeared to be a consistent function of molecular size without striking peaks (which would have suggested local articular synthesis and release) or valleys (which would have suggested specific exclusion or local articular consumption).

The pattern was somewhat different in the 16 pathological effusions. Although the diagnoses in this group were diverse, disease-related pattern differences were not obvious, and no diagnostic subset was large enough to warrant specific analysis. All tracings were therefore averaged in the same fashion as the normal data (Figure 2). As would be expected, the total protein levels in these effusions,  $4160 \pm 340$  mg/dl, were higher and displayed a wider variance than those in aspirates from "normal" subjects,  $1670 \pm 170$  mg/dl. Again, there was a progressive fall in the ratio as protein size increased. A shoulder on the initial downslope implied either widening of the smallest endothelial aperture from 1.75 nm in normal individuals to 3.5 nm in those with arthritis or local synovial release of unidentified products having  $mr$  between 2 and 3 nm. Values then fell until they reached ~7.1 nm, where they began a plateau extending up to ~9.7 nm. As in the normal data, SF concentrations of proteins larger than ~9.7 nm then rose modestly.

**Clearance.** The experimental SF/S values were multiplied by the lymphatic efflux rates to yield continuous clearance curves between 1 and 12 nm as described (Figures 3 and 4). These data were then subjected to empirical "curve stripping," which assumed that proteins leave the vasculature by 3 differing but parallel pathways. Derived curves based on this model of transmural protein traffic were then produced in accord with the concepts and methodology of Rippe and Haraldsson<sup>15</sup>.

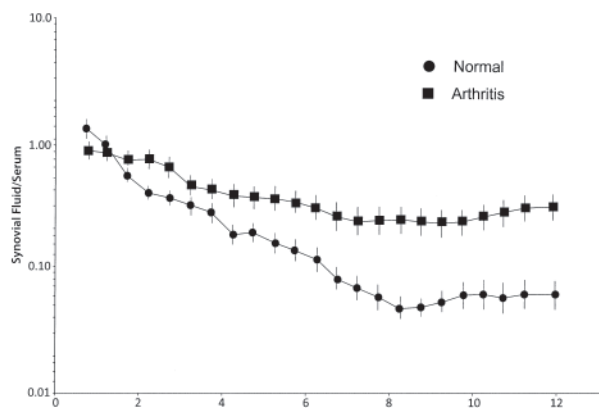


Figure 2. Mean synovial fluid/serum ratios ( $\pm$  SEM) at 23 ascending molecular radii from normal and arthritic knees.

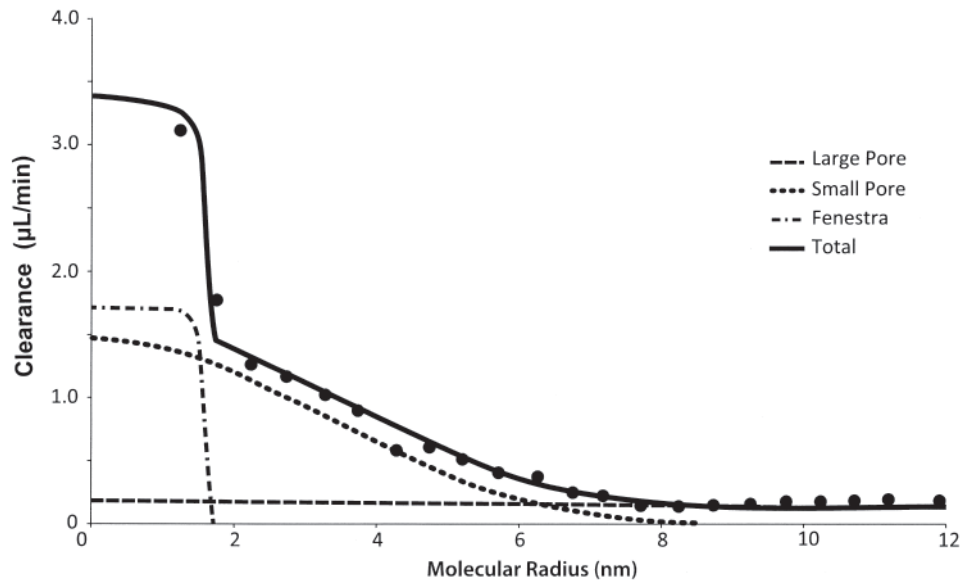


Figure 3. Mean protein clearance values at 0.5 nm intervals from normal knees (black circles) plotted against the molecular radii and analyzed by curve stripping. A 3-pore model was assumed, and curves for large, small, and fenestral pores were sequentially fitted to the experimental data. The total curve is the sum of the net filtration through the 3 apertures.

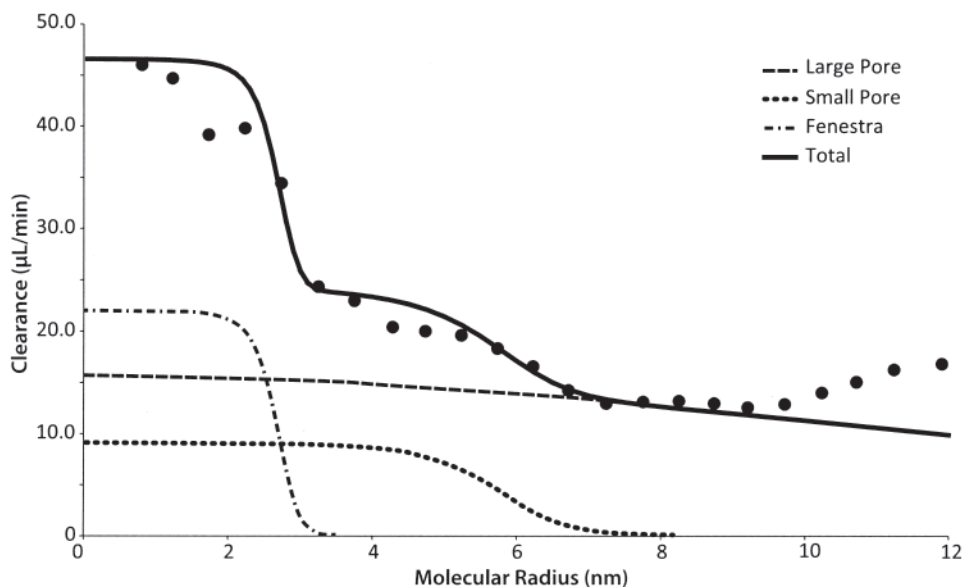


Figure 4. Large, small, and fenestral pathways through the microvascular endothelium in arthritic joints are sequentially dissected in the same fashion as in Figure 3.

These curves represent protein clearance through “large,” “small,” and “fenestral” pores. In this process, a curve was first fitted through the lowest points in the experimental data and the calculated large-pore clearance was “stripped” (subtracted) from all the datapoints, thus eliminating all proteins with radii too large to pass through the smaller apertures. This yielded a residual curve representing the sum of small-pore and fenestral clearances. The process was repeated by fitting

and stripping the small-pore portion of this summation curve, thus leaving a remainder that was taken to represent clearance through the fenestrae. The total clearance is the summation of the large, small, and fenestral curves as seen in Figures 3 and 4. For each pore, the intercept with the vertical axis indicates the net transmurial water flow through that pore, while the intercept with the horizontal axis shows its radius. These findings then permit calculation of the filtration fraction: the net

flow of plasma water through each pore at a plasma flow of 2 ml/min<sup>13</sup>. This flow rate, like those used for normal and arthritic lymphatic drainage, is based on mean observations in previous studies. Thus, the derived rates are representative, and individuals will vary. The pore size estimates, however, should not vary since they rest primarily on the SF/S determinations in this work. These results are shown in Table 1.

Both the “normal” and the “arthritic” datasets fit the model, although the “normal” is clearly tighter. Correlation coefficients between the observed clearance points and the derived values for total clearance at the same radii were 0.992 for the “normal” data and 0.980 for the “arthritic” points, with respective R<sup>2</sup> of 0.985 and 0.960.

## DISCUSSION

Our data fit a model in which molecules move from plasma into SF through 3 distinct and parallel pathways. In normal synovial microvessels, the radii of these apparent apertures were determined to be 1.75 nm, 8.6 nm, and 40 nm, while in arthritic knees they were 3.5 nm, 8.5 nm, and 36 nm.

*The pores.* In all living tissues, the microvasculature delivers oxygen and nutrient molecules while it concurrently clears carbon dioxide and other metabolic wastes. At the same time, the cellular constituents of blood as well as most of its proteins are retained within the perfusing plasma stream. This dual role of facile delivery with coextensive retention has classically been analyzed in terms of size-selective “pores” within the endothelial wall<sup>16,17</sup>.

The junctions between adjacent endothelial cells provide the most obvious candidate pores. Adjacent cells are now known to attach to each other primarily through VE-cadherin molecules at their margins. Such connections provide “adherence at arm’s length” in a zipper-like arrangement that permits paracellular passage of solutes while still maintaining a firm intercellular bond<sup>18,19</sup>. Under the electron microscope, these pathways appear to be ~20 nm in width, but they are further restricted by occludens baffles (“junction strands”) within the intercellular cleft<sup>20</sup>. Such junctions are seen in most microvessels, including the continuous capillaries of muscle, peritoneum, etc., which lack the fenestra found in synovial vessels.

Physiologically, the cadherin apertures have been thought to comprise a “small pore” pathway with a functional radius between 3 and 10 nm. These widely diverse estimates were reached with a variety of methods in differing species and tissues, but most of them rest on observed partitioning of rela-

tively few selected proteins between plasma and lymph or tissue fluid. In each study, protein markers were chosen for convenience and ease of measurement, and their choice necessarily left irregular gaps throughout the physiologic range of protein sizes. In contrast, our method includes the optical densities of all plasma proteins averaged over twenty-three 0.5-nm intervals between 1 and 12 nm.

Our mean radius of 8.6 nm is at the upper end of the estimates of others and is considerably larger than the consensus value of ~4 nm cited by Levick and Michel in their recent review of newer permeability concepts in capillary beds<sup>21</sup>.

The fenestrations of synovial microvessels present an additional pathway, a task they have been assigned because their presence here (as in the gut, renal interstitium, etc.) correlates with high permeability to water and other small molecules<sup>22</sup>. In line with this concept, we believe that the highly symmetrical, transsynovial exchange of small molecules found in our previous studies of normal human knees represents diffusive interchange across these structures<sup>1</sup>.

In an early analysis of published SF/S data for specific plasma proteins, Levick suggested that the “endothelial pore” might have a radius of ~5 nm and did not distinguish between the transcellular fenestrae and the paracellular “small pores” at the cadherin junctions<sup>7</sup>. This is not surprising since at that time there were no partitioning data for molecules with  $mr < 3$  nm. Our work expands the known range to include the critical gap between 1 and 3 nm. The fenestrae appear to be the site of our 1.75 nm pore. The small proteins that may follow this path are physiologically important because they include proteinaceous hormones, cytokines, growth factors, etc.

Previous studies of other vascular beds have consistently recognized “large pores” possessing radii of 25 nm or more. Controversy persists as to whether these convective channels in normal endothelia represent transcellular chains of interconnected, vesicular “caveolae” or whether they are unzipped segments of intercellular cadherin junctions. There is no question, however, that the latter mechanism explains the marked influx of large proteins that occurs with synovial inflammation<sup>23,24</sup>.

*Solute determinants.* The excellent fit of our data with a simple 3-pore model implies that size alone determines the rate of entry for the great majority of proteins into normal synovial fluid. We did not find clear, anomalous peaks or valleys that would have suggested respective local synthesis or endothelial exclusion. One possible exception is haptoglobin, which

Table 1. Dimensions of and flow through synovial microvascular pores.

Pore Type	Pore Radius, nm		Vascular Efflux, $\mu$ l/min		Flow Ratio Effused/normal	Filtration Fraction, %	
	Normal	Effused	Normal	Effused		Normal	Effused
Fenestra	1.75	3.5	1.74	22.0	12.6	0.087	1.10
Small pore	8.6	8.5	1.50	9.1	6.1	0.075	0.46
Large pore	40	36	0.24	15.5	64.6	0.012	0.78

nm: nanometers.

has been thought to have limited access to the joint space on the basis of its high negative-charge density<sup>25,26</sup>. In fact we did find a minor dip that corresponds well to the 4.5-nm radius of this protein. Conversely, synovial synthesis (of lubricin, for instance) clearly occurs, but the abundance of plasma proteins of comparable size made this inapparent. Over all, although minor exceptions no doubt occur, the great preponderance of plasma proteins move passively along the endothelial sieve, where their escape is sorted on a size-dependent basis unaffected by charge or by specific transport systems.

*The glycocalyx.* Recent refinements in electron microscopic (EM) technique have revealed convincing new evidence of the lining endothelial glycocalyx<sup>21,27</sup>. The existence of this ruthenium red-staining layer was well known, but it is destroyed by conventional EM fixation techniques and its structure was uncertain and underappreciated<sup>28</sup>. The lining is now known to consist of a grassy surface of proteoglycan filaments 200 nm or more in length. These filaments, composed primarily of heparan sulfate (but also containing chondroitin sulfate and hyaluronan), are thought to overhang the intercellular clefts where they may be significant determinants of small-pore paracellular permeability.

In microvessels of the gut and the renal interstitium, bush-like plugs of longer filaments, 300–400 nm in length, dubbed the fascinae fenestrae, have been found to overlie each fenestra<sup>29</sup>. The special techniques required to demonstrate these structures have not been used as yet to examine synovial vessels. It is also unknown whether the composition of the fenestral tufts differs from that of the surrounding endothelial glycocalyx, although studies with cationized markers imply that this “fuzzy coat” is thicker and possesses a more intensely negative charge over the fenestrae<sup>30</sup>. If, as seems likely, comparable structures occur in synovial vessels, this tissue will afford an ideal site to determine further the effect of their unique structure and intense charge on overall microvascular permeability.

*The synovial site.* The synovial circulation presents a number of advantages for studies of microvascular function. Since there is no lining mesothelium and no underlying basement membrane, molecules passing between or through synovial lining cells move directly between the cavity and the interstitium<sup>31</sup>. When radiolabeled albumin is injected into the knee, it mixes readily not only with the free SF but also throughout the available intracapsular volume<sup>12</sup>. Thus, the accessible fluid may be taken as representative of the interstitial fluid of the entire synovial organ.

Further, in this single tissue, served by a single fenestrated microvascular bed, physiological observations are not confounded by interstitial admixtures from adjacent muscle, skin, or other local tissues, as they are in classic study sites such as the hind limbs of dogs. Perhaps most importantly, the synovial fluid can be sampled in unanesthetized ambulatory humans without physical or pharmacological interventions to alter its vascular inflow or its lymphatic outflow. Finally, the wide

variety of synovial inflammatory diseases presents unique opportunities for investigation of the vascular pathophysiology of arthritis as well as the pharmacodynamics of its therapy.

Hyaluronan confers the characteristic viscosity of synovial fluid and is thought to play important roles in stabilizing and lubricating the joint. This megamolecule also excludes other large molecules from a modest fraction of the total fluid volume and that fraction is thus not “available” for full articular distribution of plasma proteins. However, this concern primarily affects the largest plasma proteins (a 3-fold variation in hyaluronan concentration did not affect albumin kinetics in the canine knee<sup>32</sup>), and we had no data on the concentration or the quality, i.e., chain length, of this polymer in the SF of our subjects. Further, the effect of hyaluronan (as well as other glycosaminoglycans, proteoglycans, collagens, etc.) on interstitial protein distribution could not be ascertained. Therefore, we recognize that our volume is that available to most proteins but do not attempt to correct for steric exclusion within the articular fluid.

*Vascular changes in arthritis.* In our study, we were not surprised to find a marked ~65-fold increase in the large-pore permeability of the “arthritic” vasculature. A long list of inflammatory mediators, well represented in clinical synovial effusions, has long been known to widen and open the clefts between adjacent endothelial cells<sup>23,24</sup>. This widening results from activation of the actin cytoskeleton, causing endothelial cell contraction that disrupts the VE-cadherin junctions. Our data shed no new light on the mechanism of this gap formation, but they do represent the first, specific quantification of the resultant protein efflux.

The apparent widening of the small fenestral pore from 1.75 to 3.5 nm was an unanticipated finding of this work. On closer analysis, this change appeared to be a shoulder on the clearance curve that could be further dissected out as a broad peak of small proteins around a radius of 2.2 nm. The constituents of this curve remain unknown. They could represent breakdown products of the inflammatory response or even one or more new proteins synthesized and released within the inflamed tissue. It is also possible, however, that inflammation causes shedding or disruption of the fenestral glycocalyx, and this damage then leads to increased porosity<sup>33</sup>. The prominent 12.6-fold increase in fenestral clearance seems consistent with this interpretation of possible cytokine-induced injury as an explanation for altered permeability.

In contrast to the fenestral change, the dimensions of the presumed paracellular small-pore pathway did not enlarge with inflammation, and its 6.1-fold increase in flow was less than that found for each of the other pores. Nevertheless, this change in the absence of increased plasma flow or enlarged pore dimensions implies a prominent enhancement of small-pore filtration. Increased vascular permeability is considered to be a hallmark of inflammation wherever it is found. Since the classic studies of Landis and others, this change has been attributed to the opening of paracellular large pores, but our

work indicates that other pathways increase as well. We suspect that the evident increased filtration we find across the fenestrae and the small pores primarily reflects increased oncotic pressure in the investing interstitial tissue, although increased intravascular pressure could also be involved<sup>34</sup>.

**Biomarkers.** In addition to proteins from plasma, SF can be expected to contain additional molecules from the cells of adjacent cartilage and synovium. This likelihood has generated numerous proteomic studies based on the hope that such molecules will provide useful insights into the pathogenesis of specific joint diseases<sup>35,36,37,38</sup>. Such biomarkers cannot be expected to be abundant since all input of cartilage-derived or tissue-derived molecules takes place against a high background traffic of plasma proteins. Any tissue-derived proteins can be expected to share the common efflux path and rapid turnover rates of those derived from plasma.

In practice, many candidate biomarkers are found in serum as well as SF, and the question arises whether their presence reflects passive exchange with plasma or local production and release. Because of the wide heterogeneity between and within patient groups, no existing data can be used to answer that question for a candidate protein in a given patient. We are struck, however, by the linearity of the log SF/S versus radius plots in the range between 3 and 9 nm, where most plasma proteins are found. Comparable linearity was found by Kushner and Somerville, who determined SF/S ratios for orosomucoid, transferrin, ceruloplasmin, and alpha<sub>2</sub> macroglobulin in 4 different patient groups and plotted their mean values against the log of the mw<sup>39</sup>. In view of this linearity, we suggest that serum and SF concentrations of albumin and alpha<sub>2</sub> macroglobulin may be determined in each pair of samples, the derived SF/S values can then be plotted against their respective radii of 3.5 and 9.1 nm, and the 2 points connected by a straight line. The SF/S for a candidate biomarker within this size range (which is also the realm of small-pore selectivity) may then be added if its radius is known. Points falling significantly above the connecting line will imply articular release, while those below will suggest local consumption or endothelial exclusion.

Although endogenous albumin and alpha<sub>2</sub> macroglobulin can thus provide anchors for a reference line to query possible production or release of a candidate biomarker, no evaluation based on concentration alone can determine the rates of these processes. At present, such information can come only from a concurrent assessment of the lymphatic clearance rate using labeled albumin or a comparable reference molecule. Although such determinations are feasible, they clearly add greatly to the cost and complexity of any study of biomarker candidates.

**Aquaporins.** The most studied microvascular bed in human beings is that of the peritoneum<sup>40,41,42</sup>. There, permeability is also thought to depend on a 3-pore system, but the structure is considerably different. Instead of fenestrae, "aquaporin" channels (specifically, AQP1) have been assigned the role of high-

flow delivery of water. Like the fenestrae, these apertures are transcellular paths, but unlike the fenestrae they limit passage to water alone<sup>43</sup>. By microarray analysis, aquaporin proteins have been recognized in many human tissues, and AQP1 was found to be moderately expressed in synovial endothelial cells (as well as synoviocytes and chondrocytes)<sup>44</sup>. In normal synovial vessels, we feel that aquaporins are unlikely to constitute a significant "fourth pore" because the net synovial influx of water (3.48  $\mu$ l/min) was precisely accounted for by the sum of that through large, small, and fenestral pores.

In contrast, the sum of inflow through the same 3 pores in arthritic joints (46.6  $\mu$ l/min) leaves 10.4  $\mu$ l/min of inflow unexplained. In rheumatoid joints, AQP1 was not only present but also significantly upregulated in all tissues, including the microvessels<sup>45</sup>. Given the heterogeneity of our arthritic group, the data suggest that aquaporin inflow may be a significant constituent of many synovial effusions. Clearly, this potential pathway remains an important prospect for future studies of synovial microvascular function.

We have used gel filtration chromatography of paired serum and SF specimens from normal and inflamed human knees together with known measures of lymphatic efflux and synovial plasma flow to evaluate the permeability of synovial microvessels to plasma proteins. Our data fit well with a normal 3-pore model consisting of small fenestral apertures (1.75 nm), larger paracellular clefts (8.6 nm), and large-pore nonselective gaps of 36 nm or more. These consistent dimensions imply a well organized endothelial barrier that provides essentially uniform pore sizes within and between individuals<sup>29,40,46</sup>. Size, rather than charge, appears to determine the rate at which most plasma proteins move past this barrier and into the joint.

When arthritis supervenes, the fenestral pore appears to widen either as a result of damage to the lining glycocalyx or from synovial release of inflammatory byproducts. The paracellular clefts remain unchanged, and the large pores open to permit a ~65-fold increase in the influx of larger proteins. Net filtration also increases through the fenestrae and the paracellular small pores and "water-only" aquaporin channels may function as a significant fourth pore.

## ACKNOWLEDGMENT

We are indebted to Alan Fantel, PhD, who graciously allowed us to use his chromatographic equipment, to Cynthia Johnson, who ran the column separations, and to the patients who participated in this work and in the previous kinetic studies supporting this analysis.

## REFERENCES

1. Simkin PA, Pizzorno JE. Transynovial exchange of small molecules in normal human subjects. *J Appl Physiol* 1974;36:581-7.
2. Wallis WJ, Simkin PA, Nelp WB. Protein traffic in human synovial effusions. *Arthritis Rheum* 1987;30:57-63.
3. Rodnan GP, MacLachlan MI. The absorption of serum albumin and gamma globulin from the knee joint of man and rabbit. *Arthritis Rheum* 1960;3:152-7.
4. Brown DL, Cooper AG, Bluestone R. Exchange of IgM and

- albumin between plasma and synovial fluid in rheumatoid arthritis. *Ann Rheum Dis* 1969;29:644-51.
5. Slivinski AJ, Zvaifler NJ. The removal of aggregated and nonaggregated autologous gamma globulin from rheumatoid joints. *Arthritis Rheum* 1969;12:504-14.
  6. Bauer W, Ropes MW, Waite H. The physiology of articular structures. *Physiol Rev* 1940;20:272-312.
  7. Levick JR. Permeability of rheumatoid and normal human synovium to specific plasma proteins. *Arthritis Rheum* 1981;24:1550-60.
  8. Simkin PA, Bassett JE. Synovial fluid protein concentrations vary among normal human joints [abstract]. *Arthritis Rheum* 1989;32 Suppl:S16.
  9. Platt D, Pigman W, Holley HL, Patton FM. An electrophoretic study of normal and post-mortem human and bovine synovial fluids. *Arch Biochem Biophys* 1956;64:152-63.
  10. Schur PH, Sandson J. Immunologic studies of proteins of human synovial fluid. *Arthritis Rheum* 1963;6:115-29.
  11. Andrews P. Estimation of molecular size and molecular weights of biological compounds by gel filtration. *Methods Biochem Anal* 1970;18:1-53.
  12. Wallis WJ, Simkin PA, Nelp WB, Foster DM. Intraarticular volume and clearance in human synovial effusions. *Arthritis Rheum* 1985;28:441-9.
  13. Myers SL, Brandt KD, Eilam M. Even low-grade synovitis significantly accelerates the clearance of protein from the canine knee. *Arthritis Rheum* 1995;38:1085-91.
  14. Simkin PA, Bassett JE, Koh EM. Synovial perfusion in the human knee: A methodological review. *Semin Arthritis Rheum* 1995;25:56-66.
  15. Rippe B, Haraldsson B. Transport of macromolecules across microvascular walls: The two-pore theory. *Physiol Rev* 1994;74:163-219.
  16. Pappenheimer J. Passage of molecules through capillary walls. *Physiol Rev* 1953;33:387-423.
  17. Renkin EM. Capillary transport of macromolecules: pores and other endothelial pathways. *J Appl Physiol* 1985;58:315-25.
  18. Vincent PA, Xiao K, Buckley KM, Kowalczyk AP. VE-cadherin: adhesion at arm's length. *Am J Physiol Cell Physiol* 2003;286:C987-97.
  19. Vestweber D. VE-cadherin. The major endothelial adhesion molecule controlling cellular junctions and blood vessel formation. *Arterioscler Thromb Biol* 2008;28:222-32.
  20. Firth JA. Endothelial barriers: From hypothetical pores to membrane proteins. *J Anat* 2002;200:541-8.
  21. Levick JR, Michel CC. Microvascular fluid exchange and the revised Starling principle. *Cardiovasc Res* 2010;87:198-210.
  22. Levick JR, Smaje LH. An analysis of the permeability of a fenestra. *Microvasc Res* 1987;33:233-56.
  23. Kumar P, Shen Q, Pivetti CD, Lee ES, Wu MH, Yuan SY. Molecular mechanisms of endothelial hyperpermeability: implications in inflammation. *Expert Rev Mol Med* 2009;11:e19.
  24. DiStasi MR, Ley K. Opening the flood-gates: how neutrophil-endothelial interactions regulate permeability. *Trends Immunol* 2009;30:547-56.
  25. Nettelbladt E, Sundblad L, Jonsson E. Permeability of the synovial membrane to proteins. *Acta Rheumatol Scand* 1963;9:28-32.
  26. Nettelbladt E, Sundblad L. Haptoglobins in serum and synovial fluid. *Acta Rheumatol Scand* 1965;11:11-4.
  27. Weinbaum S, Tarbell JM, Damiano ER. The structure and function of the endothelial glycocalyx layer. *Annu Rev Biomed Eng* 2007;9:121-67.
  28. Luft JH. Fine structure of capillary and endocapillary layer as revealed by ruthenium red. *Fed Proc* 1966;25:1773-83.
  29. Rostgaard J, Qvortrup K. Electron microscopic demonstrations of filamentous molecular sieve plugs in capillary fenestrae. *Microvasc Res* 1997;53:1-13.
  30. Simionescu M, Simionescu N. Functions of the endothelial surface. *Ann Rev Physiol* 1986;48:279-93.
  31. Levick JR. Blood flow and mass transport in synovial joints. In: *Handbook of physiology, cardiovascular system IV, the microcirculation*. Renkin EM, Michel CC, editors. Bethesda, MD: American Physiological Society; 1984:917-47.
  32. Myers SL, Brandt KD. Effects of synovial fluid hyaluronan concentration and molecular size on protein clearance from the canine knee. *J Rheumatol* 1995;22:1732-9.
  33. Speziale S, Sivaloganathan S. Poroelastic theory of transcapillary flow: Effects on endothelial glycocalyx deterioration. *Microvasc Res* 2009;78:432-41.
  34. McDonald JN, Levick JR. Effect of extravascular plasma protein on pressure-flow relations across the synovium in anaesthetized rabbits. *J Physiol* 1993;465:539-59.
  35. Gibson DS, Rooney ME. The human synovial fluid proteome: A key factor in the pathology of joint disease. *Proteomics Clin Appl* 2007;1:889-99.
  36. Gobeze R, Kho A, Krastins B, Sarracino DA, Thornhill TS, Chase M, et al. High abundance synovial fluid proteome: distinct profiles in health and osteoarthritis. *Arthritis Res Ther* 2007;9:R36.
  37. De Ceuninck F, Berenbaum F. Proteomics: Addressing the challenges of osteoarthritis. *Drug Discovery Today* 2009;14:661-7.
  38. Baillet A, Trocme C, Berthier S, Arlotto M, Grange L, Chenau J, et al. Synovial fluid proteomic footprint: S100A8, S100A9 and S100A12 proteins discriminate rheumatoid arthritis from other inflammatory joint diseases. *Rheumatology* 2010;49:671-82.
  39. Kushner I, Somerville A. Permeability of human synovial membrane to plasma proteins: relationship to molecular size and inflammation. *Arthritis Rheum* 1971;14:560-70.
  40. Rippe B, Rosengren B-I, Venturoli D. The peritoneal circulation in peritoneal dialysis. *Microcirculation* 2001;8:303-20.
  41. Flessner MF. Endothelial glycocalyx and the peritoneal barrier. *Perit Dial Int* 2008;28:6-12.
  42. Nishino T, Devuyt O. Clinical application of aquaporin research: aquaporin-1 in the peritoneal membrane. *Pflugers Arch - Eur J Physiol* 2008;456:721-7.
  43. Zeuthen T. Water-transporting proteins. *J Membrane Biol* 2010;234:57-73.
  44. Mobasheri A, Marples D. Expression of the AQP-1 water channel in human tissues: A semiquantitative study using tissue microarray technology. *Am J Cell Physiol* 2004;286:C529-37.
  45. Trujillo E, Gonzalez T, Marin R, Martin-Vasallo P, Marples D, Mobasheri A. Human articular chondrocytes, synoviocytes, and synovial microvessels express aquaporin water channels; upregulation of AQP1 in rheumatoid arthritis. *Histol Histopathol* 2004;19:435-44.
  46. Squire JM, Chew M, Nneji G, Neal C, Barry J, Michel C. Quasi-periodic substructure in the microvessel endothelial glycocalyx: a possible explanation for molecular filtering? *J Struct Biol* 2001;136:239-55.